Optimization of coagulation treatment process for the removal of refractory organics from leachate concentrate

Qianru Wu, Hui Ji, Na Wei, Wenqiang Wang*

College of Chemistry and Chemical Engineering, Dezhou University, Dezhou 253023, China, emails: wwqzs@126.com (W. Wang), 1277538873@qq.com (Q. Wu), 1435506240@qq.com (H. Ji), 3225585982@qq.com (N. Wei)

ABSTRACT

High concentrations of refractory organics contained in leachate concentrates (LC) must be removed to mitigate their threat to the environment. In this work, effective removal of refractory organics from LC was performed using the $FeCl_3$ coagulation process. The coagulation process was optimized using the response surface method, and the highest chemical oxygen demand (COD), chromaticity, and UV_{254} removal efficiencies were 61.48%, 89.74%, and 76.59%, respectively, under optimal conditions, $FeCl_3$, 1.8 g/L; PAM, 2.0 mg/L; and pH 5. $FeCl_3$ dose and pH were the main influencing factors on COD removal. The COD concentration in the LC was reduced from 1,240 to 478 mg/L, and the biodegradability of the LC was improved by coagulation. Fourier transform infrared and spectrophotometric analyses showed that the majority of organic matter was humic acid and was effectively removed by coagulation.

Keywords: Leachate concentrate; Coagulation; Response surface method

1. Introduction

Reverse osmosis (RO) and nanofiltration (NF) have been widely used for advanced treatment of landfill leachate due to their advantages, including easy operation, no added chemicals, low energy requirements, and removal of almost all of the soluble substances [1,2]. However, the generation of large volumes of leachate concentrate (LC), which accounts for typically 10%–30% of the influent volume [3], is one of the major issues with these processes. LC contains high concentrations of refractory organics (e.g., humic substances, aromatic compounds, and halogenated hydrocarbons), heavy metals, and inorganic salts. LC is more difficult to treat compared to the original leachate due to a higher content of refractory organics, higher salinity, higher chromaticity, and lower biodegradability [4]. Therefore, the proper treatment of LC to reduce its large negative impacts on the environment is necessary.

Currently, common treatments for LC mainly include recirculation [5], membrane separation [6], evaporation [7], adsorption [8], coagulation [9,10], and advanced oxidation processes (AOPs) [11–13]. However, these methods have their own drawbacks. Recirculation can result in an accumulation of pollutants. Evaporation requires large amounts of land and high operational costs, along with poor stability and equipment corrosion. Adsorption and membrane separation processes do not destroy the pollutants in LC, but merely take them away from the LC. In most cases, AOPs can only mineralize small fractions of organics and require specific conditions including high oxidant dosages, high-intensity energy input, and long reaction times [14].

Coagulation process as an effective conventional method has been widely used to treat the industrial wastewaters for the removal of organic pollutants [15–17]. For LC treatment, coagulation is also economically viable and effective. It can remove refractory organics in LC and improve the biodegradability of LC [18]. The values of chemical oxygen

---

* Corresponding author.

demand (COD) and ammonia nitrogen in water samples after coagulation treatments were 88 and 10.8 mg/L, respectively, which met the standard in the Pollution Control Standard of Domestic Refuse Landfill GB 16889–2008 [19]. The molecular compositions and changes of dissolved organic matter in LC after coagulation with Al or Fe sulfate were characterized using electrospray ionization coupled with Fourier transform ion cyclotron resonance mass spectrometry and unsaturated (H/C < 1.0) and oxidized (O/C > 0.4) substances containing carboxyl groups were preferentially removed after coagulation [9]. Coagulation process reduced the adverse impact of high-molecular-weight organic matters such as humic acids, on the aerated internal micro-electrolysis process for the treatment of NF concentrate from mature landfill leachate [20]. The coagulation conditions, except for the type of coagulant, including the coagulant dosage, pH, reaction time, also affect the organics removal efficiency; therefore, determination of the optimum coagulation conditions is necessary to obtain the optimum pollutant removal efficiency.

One of the methodologies for obtaining the optimum results is the response surface methodology (RSM) which involves the reduced number of experimental trials needed to evaluate multiple parameters and their interactions. The objective of the present study was to evaluate the removal of refractory organics from the LC by coagulation. The coagulation process was designed and optimized using RSM. The Box–Behnken design (BBD) was used to define the conditions of independent variables providing maximum organics removal efficiency. In addition, changes in organics composition, biodegradability, and coagulation mechanisms were also investigated.

2. Materials and methods

2.1. LC

The LC was collected from a municipal solid waste landfill site located in Dezhou, China. The age of the landfill is approximately 10 y. The LC was treated by a combined anoxic/oxic-membrane bioreactor-RO process. The characteristic properties of the LC are listed in Table 1.

2.2. Experimental methods

Coagulation experiments of the LC were performed in beakers using a program-controlled jar test apparatus with six paddles. It has been established that iron salts are more efficient than aluminum salts [21] and that the addition of flocculant and coagulant together may enhance the floc-settling rate [22]. Moreover, $FeCl_3$ is more efficient than other iron salts for the treatment of LC [10]. Therefore, in the present study, $FeCl_3$ and polyacrylamide (PAM) were selected as the coagulant and coagulant aid, respectively. The influence factors, including $FeCl_3$ and PAM amounts, pH values, and settling times were studied by varying any one of the process parameters and holding the other parameters constant. The LC pH was adjusted using 2 M H_2SO_4 or 10 M NaOH before coagulation. In the coagulation process, 1 min of rapid stirring (200 rpm), subsequent 15 min of slow stirring (50 rpm), and final 6 h of settling time were

Table 1
Characteristics of the LC

Parameters	Average value
pH	7.40
COD (mg/L)	1,240
BOD_5 (mg/L)[a]	113.8
UV_{254} (cm^{-1})[b]	18.816
Chromaticity (dilution)	1,950
Conductivity (ms/cm)	68.88
TOC (mg/L)	452
TDS (g/L)[c]	57.90

[a]BOD_5, biochemical oxygen demand; [b]UV_{254} ultraviolet; [c]TDS, total dissolved solids.

performed, and the supernatant was collected for COD, BOD_5, UV_{254}, and chromaticity measurements.

The $FeCl_3$ dosage, PAM dosage, and pH were chosen on the basis of preliminary experiments to perform RSM experiments. BBD is among the principal response surface methodologies used in the experimental design and was used to optimize the three main factors in the coagulation process. The average values for two parallel experiments were reported.

The software Design Expert 8.0 (Stat-Ease Inc., Minneapolis, USA) was employed for the planning of the experiments, input tests, the forming of a mathematical model to predict the response as a function of the independent variables involving their interactions, and drawing of the plots. Analysis of variance (ANOVA) was used for graphical analyses of the data to evaluate the interactions between the process variables and the responses [23]. The coefficient of determination (R^2) expressed the quality of the polynomial fitting model. The *P*-value (probability) with a 95% confidence level was used to check the statistical significance of the model terms. For each response, the square of the correlation coefficient was obtained as R^2. A high R^2 indicated that the model calculations agreed well with the experimental data. R^2 should be more than 0.8 for a reasonable model [24]. The predicted determination coefficient (Pred R^2) should be in reasonable agreement with the adjusted determination coefficient (Adj. R^2). The coefficient of variation (the percentage ratio of the standard deviation to the mean value, CV) was used to evaluate the reproducibility of the model. A model with a CV lower than 10% was considered to be reasonably reproducible.

2.3. Analytical methods

The COD, BOD_5, TDS, and chromaticity measurements were performed using standard methods [25]. TOC concentrations were measured using a Shimadzu TOC-Vcpn analyzer. UV_{254} was measured using a UV-visible spectrophotometer (JH752, Jinghua, China) at a wavelength of 254 nm after filtration of the samples through a 0.45 μm nylon filtration membrane. The pH was determined by a pH-meter (PHS-3C, Rex, China). Conductivity was measured using a conductivity meter (DDSJ-308F, Rex, China).

The LC treated by coagulation under optimum conditions and the raw LC samples were dried in an oven at 40°C for 48 h, and the powders were mixed with KBr and pressed into discs for Fourier-transform infrared (FT-IR) analysis (Nicolet iS50, Thermo, USA) [26]. The two samples were also used for absorbance scanning and three-dimensional fluorescence analysis. Absorbance scanning of water samples in the range 200–400 nm was performed by a Shimadzu UV-2450 spectrophotometer (Shimadzu, Kyoto, Japan). Fluorescence excitation-emission matrix (EEM) spectra were obtained using a fluorescence spectrophotometer (FLS 980, Edinburgh, UK) equipped with a 450 W xenon lamp as the steady-state excitation source. The filtered sample (3 mL) was scanned in a 1 cm quartz cell at excitation and emission ranges from 200 to 450 nm at 2 nm increments and from 200 to 550 nm at 5 nm increments, respectively. The slit was 2 nm for both excitation and emission. The samples were diluted 10 times to avoid errors associated with the inner filter effect (IFE) [27]. Origin 8.0 (Origin Lab Inc., USA) software was employed to handle the EEM data and to help identify compounds based on specific peaks.

3. Results and discussion

3.1. Coagulation studies

3.1.1. Effect of pH

The effect of pH on coagulation of the LC with 1 g/L of $FeCl_3$ was investigated in the pH range of 2–7, as shown in Fig. 1. The COD removal efficiencies initially increased, then decreased as the pH increased. The differences in the coagulation mechanisms of hydrolysis products of $FeCl_3$ under different pH values resulted in different COD removal efficiencies. At lower pH values, the majority of the Fe(III) hydrolysis product was unhydrolyzed iron ion hydrate. At higher pH values, the hydrolysis products changed to single hydroxyl complexes, hydroxyl complexes, or polymers and iron hydroxide precipitates. The COD removal efficiencies were better with an acidic pH
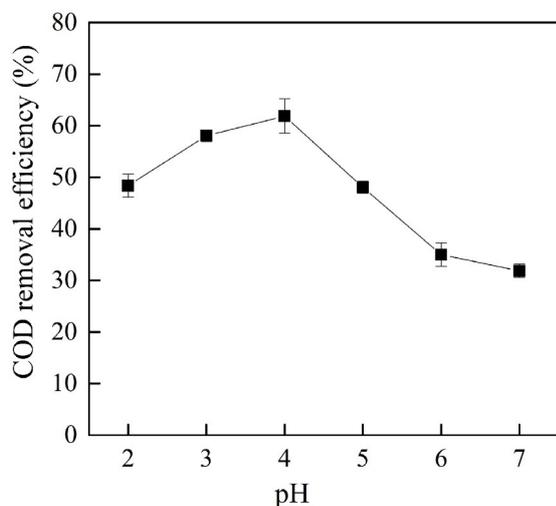
as ferric ions can hydrolyze and form polynuclear cations which are preferable over $Fe(OH)_3$ and $Fe(OH)_4^-$ formed in basic pH as nearly all colloidal impurities in water are negatively charged [28]. The suitable pH value of $FeCl_3$ in this study was 4, which was consistent with the results of Long et al. [10] and the corresponding best COD removal efficiency was 61.15%.

3.1.2. Effect of the $FeCl_3$ dosage

The effect of the $FeCl_3$ dosage on the COD removal efficiencies at the appropriate pH of 4 was evaluated. Fig. 2 shows that the COD removal efficiency rapidly increased from 21.10% to 56.53% when the $FeCl_3$ dosage was changed from 0.2 to 1.4 g/L, but slightly decreased when the dosage was increased above 1.4 g/L. The results can be explained by restabilization of colloidal particles triggered by the increasing coagulant concentration [29]. A 1.4 g/L dose of $FeCl_3$ was found to be the optimum dosage for maximum reduction of COD.

3.1.3. Effect of PAM dosage

The effect of the PAM dosage on the COD removal efficiencies at the appropriate pH of 4 and $FeCl_3$ dosage of 1.4 g/L was investigated. As shown in Fig. 3, the optimal PAM dosage was 4 mg/L, and the corresponding best COD removal efficiency was 60.81%. The COD removal efficiencies initially increased, then decreased as the PAM dosage increased. When the dosage of PAM is low, its effects are limited and it is difficult to effectively play the bridging and sweeping role of macromolecules. However, its coagulation effect is not better at higher concentrations. On one hand, when the PAM concentration is too high, its molecular chain is not fully extended and its adsorption bridging effect is weakened. On the other hand, the colloid may be completely adsorbed and covered by PAM to form a protective effect on the colloid, which is not easy to accumulate and precipitate, making the coagulation effect worse [30].
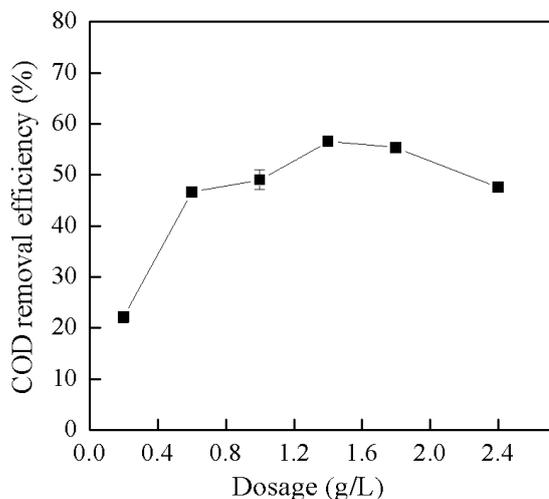

Fig. 1. Effect of pH on the COD removal efficiencies.

Fig. 2. Effect of the dosage of $FeCl_3$ on the COD removal efficiencies.

Thus, the appropriate dosage of PAM can further neutralize the negative charge on the colloid surface and fully play the adsorption bridging role to make the flocs increase and sink rapidly.

3.1.4. Effect of settling time

The effect of settling time on the COD removal efficiencies was also studied in the range of 1–24 h. The experimental observations showed that the COD removal efficiencies were not highly time-sensitive and that the 6 h settling time was actually enough.

3.2. Coagulation process optimization

3.2.1. Coagulation process removal performance

The coagulation process was optimized using the RSM to determine the optimum values of the variables of the coagulation process for achieving acceptable efficiencies of the responses. The pH (X_1), FeCl$_3$ (X_2), and PAM (X_3) dosages were taken into account as the independent variables based on the preliminary studies in Section 3.1 (Coagulation studies), and COD removal efficiency was the dependent variable. The three substantial operational parameters, as well as their low, medium, and high levels, are given in Table 2. Table 3 lists the experimental conditions and value for the response. The data in Table 3
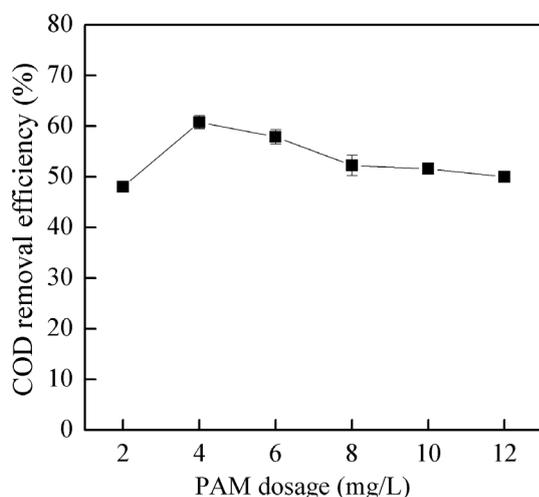
show that the highest COD removal efficiency of 61.48% were achieved at pH 5, FeCl$_3$ of 1.4 g/L, and PAM of 2 mg/L. As a result, the COD concentration of the LC was reduced from 1,240 to 478 mg/L under these conditions. Coagulation is preferred for removal of macromolecular organic matter, and a large quantity of refractory organics with low molecular weight was still retained in the coagulation effluent which needed to be further removed using other methods, such as AOPs [31].

3.2.2. Coagulation process optimization

The ANOVA results are shown in Table 4 to evaluate the combined impact of the process variables, including pH,

Table 3
Experimental conditions and results

Run	Variables			Responses
	pH	FeCl$_3$ (g/L)	PAM (mg/L)	COD removal efficiency (%)
1	4	1.4	4	47.31
2	3	1.0	4	37.23
3	5	1.4	6	59.03
4	4	1.0	6	51.77
5	3	1.8	4	43.03
6	4	1.4	4	50.21
7	4	1.8	6	43.63
8	5	1.4	2	61.48
9	4	1.0	2	44.19
10	5	1.0	4	59.61
11	4	1.4	4	51.29
12	4	1.8	2	50.81
13	3	1.4	6	41.42
14	5	1.8	4	59.85
15	4	1.4	4	49.19
16	4	1.4	4	42.39
17	3	1.4	2	28.58

Fig. 3. Effect of the dosage of PAM on the COD removal efficiencies.

Table 2
Independent variables and levels used for BBD

Variables	Coded and actual levels		
	−1	0	1
Initial pH values	3	4	5
FeCl$_3$ dosage (g/L)	1.0	1.4	1.8
PAM dosage (mg/L)	2	4	6

Table 4
ANOVA results for the COD removal efficiency

Source	Sum of squares	df	Mean square	F-value	p-value Prob > F
Model	1,143.73	6	190.62	19.20	<0.0001
X_1-pH	1,005.99	1	1,005.99	101.31	<0.0001
X_2-FeCl$_3$	2.55	1	2.55	0.26	0.6230
X_3-PAM	14.55	1	14.55	1.47	0.2539
X_1X_2	7.73	1	7.73	0.78	0.3984
X_1X_3	58.45	1	58.45	5.89	0.0357
X_2X_3	54.46	1	54.46	5.49	0.0412
Residual	99.29	10	9.93		
Lack of fit	50.25	6	8.38	0.68	0.6783
Pure error	49.04	4	12.26		

FeCl$_3$, and PAM dosages on the COD removal efficiency. Values of "Prob > F" less than 0.0500 and greater than 0.1000 indicate that the model terms are significant and not significant, respectively. The model F-value of 19.20 and P of <0.0001 implied that the model was significant. As for COD removal efficiency, X_1 was the very significant model terms. Therefore, the pH greatly affected the COD removal efficiency. When all of the insignificant terms were removed, the modified regression model for the COD removal efficiency could be represented by Eq. (1). The lack of fit F-value of 0.68 implied that the lack of fit was not significant relative to the pure error. The "Pred. R^2" of 0.7485 is in reasonable agreement with the "Adj. R^2" of 0.8722. In addition, the R^2 value of 0.9201 in Table 5 indicated that the model was able to fit at least 92.01% of the variability in COD removal efficiencies obtained from the experimental data. The CV was 6.52% (<10%), showing good reproducibility and accuracy. Adequate precision (the signal to noise ratio) of 14.87 was greater than 4 and indicated an adequate signal. Overall, the statistical analysis showed a satisfaction of the modified regression model for COD removal efficiency.

$$\text{COD removal efficiency (\%)} = 23.72X_1 + 33.76X_2 + 14.78X_3 - 3.48X_1X_2 - 1.91X_1X_3 - 4.61X_2X_3 - 77.1 \qquad (1)$$

The contour plots and three-dimensional response surfaces of the regression model can provide useful information about the interactions among independent variables and responses within the experimental design. Circular contours signify that the interactive effects between the variables are not significant and that the optimum values of the test variables cannot be easily obtained, and elliptical contours indicate that the interaction between the individual variables is significant [32]. The contour plots and response surface curves for this study are shown in Fig. 4. Fig. 4a shows that in the FeCl$_3$ dosage range 1.0–1.8 g/L, the COD removal efficiency increased with the pH, increasing from 3.0 to 5.0. Similar interactive effects between pH and PAM dosage on the COD removal efficiency could be found, as shown in Fig. 4c. It was confirmed that pH was the key factor affecting the COD removal efficiency, as had been demonstrated by ANOVA results. Fig. 4e shows that higher PAM dosages at low FeCl$_3$ dosages or higher FeCl$_3$ dosages at low PAM dosages resulted in a higher COD removal efficiency at pH 4. Fig. 4d clearly shows that the highest COD removal efficiency, 61.48%, could be achieved by adding PAM 2.0 mg/L, and FeCl$_3$ 1.4 g/L at pH 5. Based on the optimization of this model, the conditions FeCl$_3$ 1.8 g/L and PAM 2.0 mg/L at pH 5 gave a COD removal efficiency of 64.85%, which does not differ significantly from the highest experimental value, 61.48%. The optimum conditions for the coagulation process for the LC treatment were therefore pH 5, FeCl$_3$ 1.4 g/L, and PAM 2.0 mg/L and were used in subsequent experiments.

In order to lighten the interpretation of the parameter effect, Pareto analysis was applied based on Eq. (2) [33] and Pareto graph is presented in Fig. 5.

$$P_i = \left(\frac{b_i^2}{\sum b_i^2} \right) \times 100 \qquad (i \neq 0) \qquad (2)$$

Table 5
Statistical parameters from the analysis of variance for the regression models

Parameters	Values	Parameters	Values
Standard deviation	3.15	R^2	0.9201
Mean	48.30	Adjusted R^2	0.8722
C.V. %	6.52	Predicted R^2	0.7485
PRESS	312.60	Adequate precision	14.87

where P_i is the percentage effect of each variable and their combinations, b_i is the linear, quadratic or interaction coefficients in Eq. (1).

The results of Fig. 5 suggest that FeCl$_3$ and pH variables have percentage effects of 58% and 29% respectively, which produce the main effect on coagulation efficiency. The interaction effect of coagulation parameters was negligible which can facilitate the control of the process.

3.3. Analysis of the removal of organics

Under optimal conditions for COD removal, the chromaticity and UV$_{254}$ reduction efficiencies were 89.74% and 76.59%, respectively. Moreover, the ratio of BOD$_5$/COD increased from 0.09 to 0.26 after coagulation, improving the biodegradability of the LC for any possible follow-up biological treatment.

The spectrophotometric scanning spectra (200–400 nm) of the raw and treated LC are shown in Fig. 6. The pattern of the raw LC shows an absorbance peak at approximately 230 nm and a continuous decrease in absorbance in the range of 230–400 nm. The coagulation treatment led to an obvious decrease in absorbance in the entire range of 200–400 nm and the absorbance sharply decreased in the range of 230–250 nm. This pattern is consistent with the results of analysis of a high UV$_{254}$ removal by coagulation. Identifying the various fractions of the organic matter being removed in each case requires further investigation.

FT-IR and EEM spectroscopies were used to obtain information on the removal mechanisms of organic pollutants during coagulation with FeCl$_3$ at optimal experimental conditions. Analyses were performed on raw and treated LC. The absorption bands were interpreted based on literature studies [34]. As shown in Fig. 7, the IR spectra exhibited similar absorption peaks for raw and treated LC, apart from the band at approximately 1,640 cm^{-1} which was attributed to the C=O stretching vibrations in cyclic and acyclic compounds, ketones, and in quinones. The absorption peak at 1,384 cm^{-1} could be attributed to the high NO$_3^-$ concentrations. The band at 1,120 cm^{-1} was attributed to the C–O stretching of esters, ethers, and phenols. The band at approximately 3,400 cm^{-1} was attributed to OH groups. The band at 620 cm^{-1} was attributed to the phosphate group. The absorption intensity for the treated LC was weaker than that for the raw LC at the band of 3,400 and 620 cm^{-1}, which indicated the corresponding organics were removed by coagulation.

Fig. 8 shows the EEM fluorescence spectra of the raw and treated LC. There was a significant reduction in
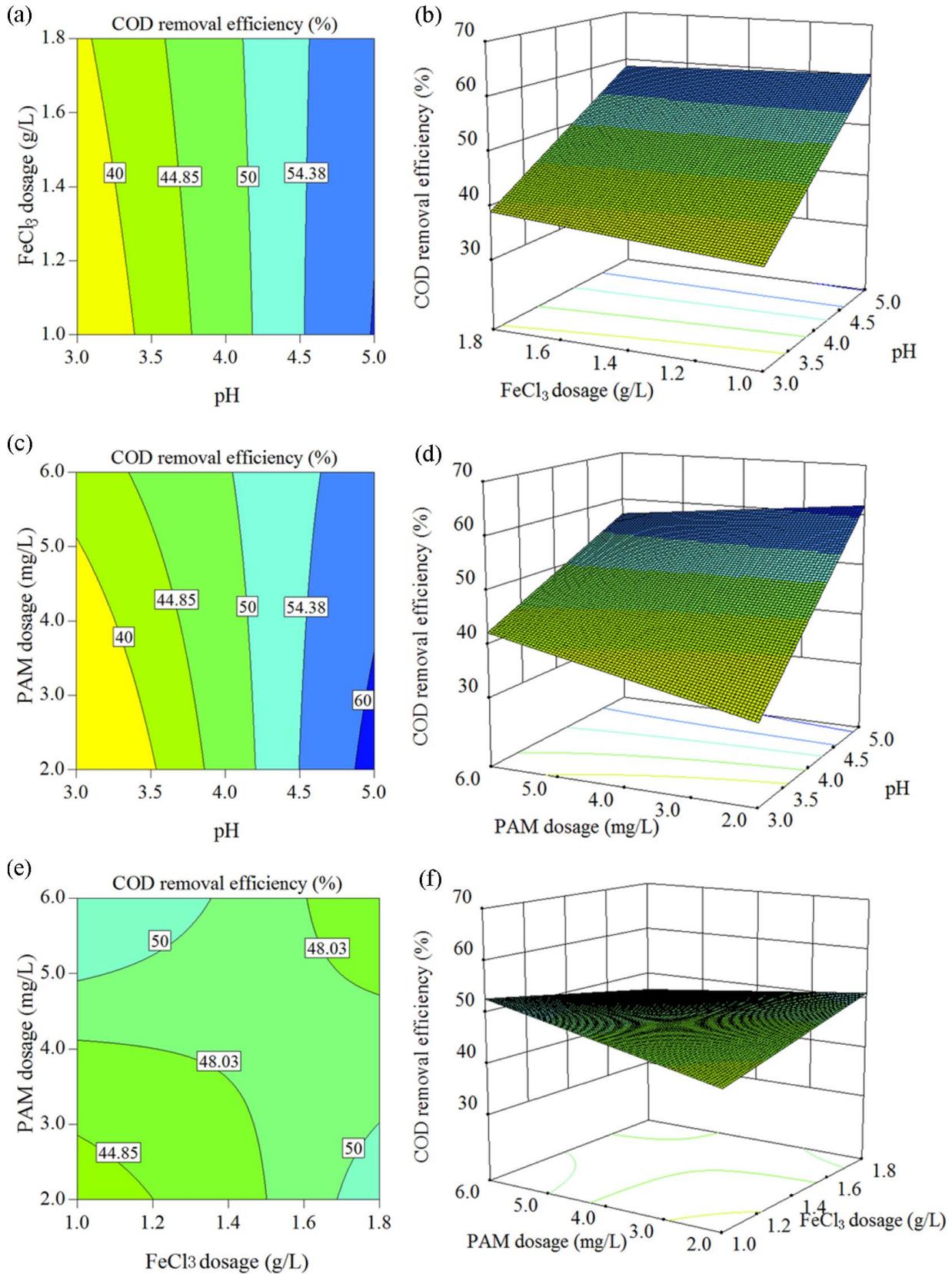
Fig. 4. Contour (a, c, e) and response surface (b, d, f) plots of the COD removal efficiency as a function of pH and the FeCl$_3$ dosage at a fixed PAM dosage (4 mg/L); pH and PAM dosage at a fixed FeCl$_3$ dosage (1.4 g/L); and FeCl$_3$ and PAM dosage at a fixed pH (4), respectively.
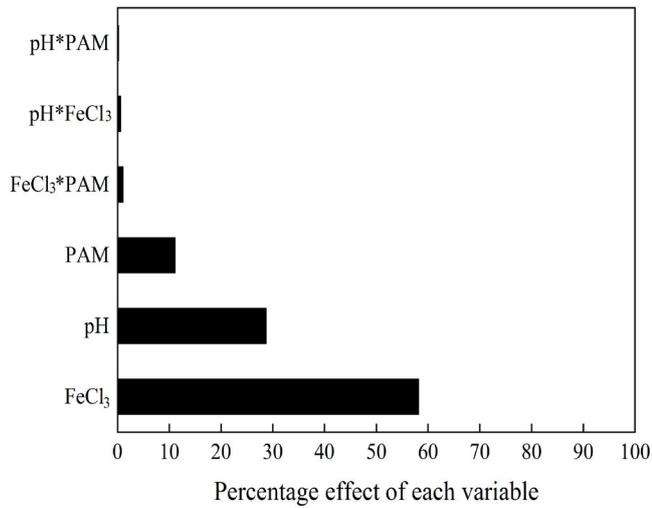
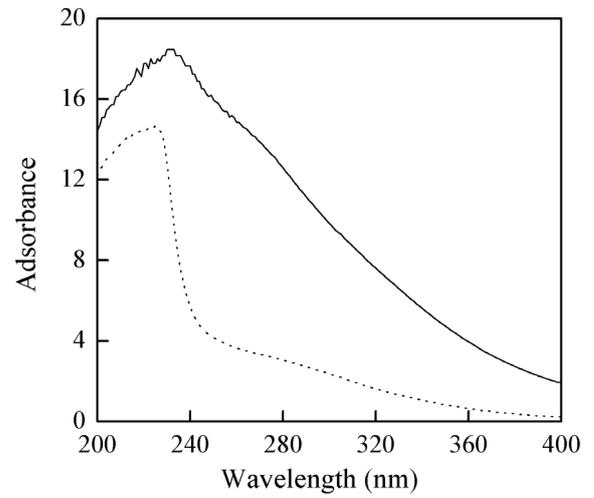Fig. 5. Pareto chart of coagulation for the percentage effect of each variable and their combinations.

Fig. 6. Spectrophotometric analysis of raw (solid) and treated (dotted) LC.
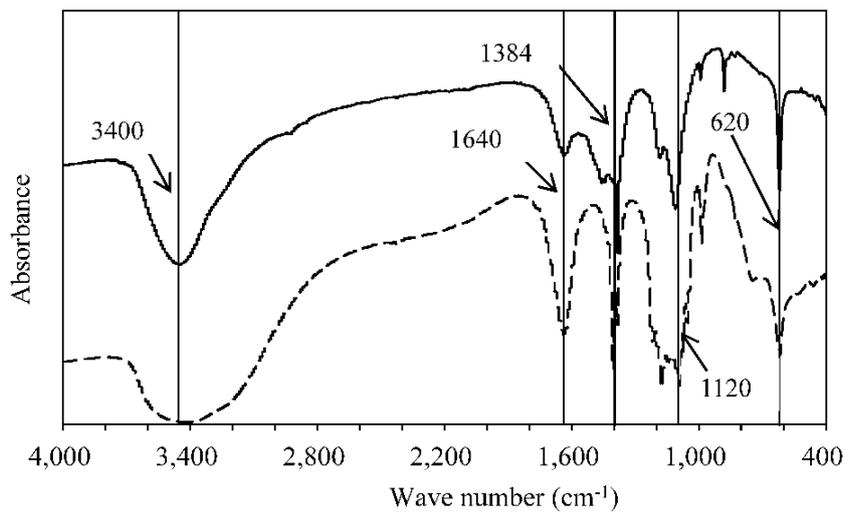

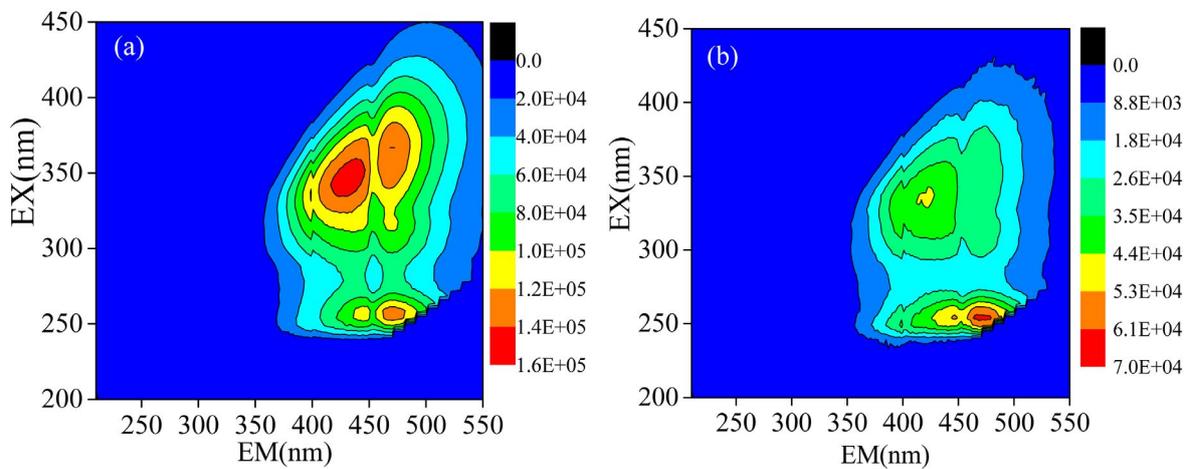Fig. 7. FT-IR analysis of raw (solid) and treated (dotted) LC.

Fig. 8. EEM spectrum of raw LC (a) and coagulation effluent (b).

fluorescence intensities for the treated LC, indicating that the organics were effectively removed by the coagulation process, although the patterns of the EEM spectra of the raw and treated ROC were similar. The results are consistent with the analysis of the spectrophotometric scanning spectra. The EEM spectra for raw LC (Fig. 8a) showed dominant responses for humic acid ($\lambda_{EX}/\lambda_{EM}$ = (325–395)/(390–500)) and weak responses for fulvic acid ($\lambda_{EX}/\lambda_{EM}$ = (220–250)/(380–480)) [35], which shows that the organics in the raw LC consisted mainly of humic acid. Humic fluorescence material removal was very difficult via biotreatment [36] and typically remained in the biologically treated effluent, for example, the influent of the RO system, and was subsequently rejected in the LC. Fig. 8b shows that more humic acid was removed by the coagulation treatment compared to fulvic acid based on the reduction in fluorescence intensities. Therefore, the majority of organic material removed by the coagulation process was humic acid.

4. Conclusions

Removal of refractory organics from LC using coagulation was examined by batch experiments and optimized using RSM in the present study. Among all factors, $FeCl_3$ dosage and the pH had the main effect on the COD removal. Under optimal conditions, $FeCl_3$, 1.8 g/L; PAM, 2.0 mg/L; and pH 5, the COD, chromaticity and UV_{254} removal efficiencies were 61.48%, 89.74%, and 76.59%, respectively. Thus, the COD concentration in LC was reduced from 1,240 to 478 mg/L. Moreover, coagulation treatments increased the ratio of BOD_5/COD from 0.09 to 0.26 and improved the biodegradability of LC. Raw LC mainly contained humic acid, which was effectively removed during the coagulation process.

Acknowledgments

References

[1] M. Ince, E. Senturk, G. Onkal Engin, B. Keskinler, Further treatment of landfill leachate by nanofiltration and micro-filtration–PAC hybrid process, Desalination, 255 (2010) 52–60.
[2] M.C.S. Amaral, W.G. Moravia, L.C. Lange, M.M.Z. Roberto, N.C. Magalhães, T.L. Dos Santos, Nanofiltration as post-treatment of MBR treating landfill leachate, Desal. Water Treat., 53 (2015) 1482–1491.
[3] O. Rodriguez, J.M. Peralta-Hernandez, A. Goonetilleke, E.R. Bandala, Treatment technologies for emerging contaminants in water: a review, Chem. Eng. J., 323 (2017) 361–380.
[4] B. Zhou, Z. Yu, Q. Wei, H. Long, Y. Xie, Y. Wang, Electrochemical oxidation of biological pretreated and membrane separated landfill leachate concentrates on boron doped diamond anode, Appl. Surf. Sci., 377 (2016) 406–415.
[5] P.S. Calabrò, E.C. Meoni, S. Orsi, D. Komilis, Effect of the recirculation of a reverse osmosis concentrate on leachate generation: a case study in an Italian landfill, Waste Manage., 76 (2018) 643–651.
[6] Y. Xu, C. Chen, X. Li, J. Lin, Y. Liao, Z. Jin, Recovery of humic substances from leachate nanofiltration concentrate by a two-stage process of tight ultrafiltration membrane, J. Cleaner Prod., 161 (2017) 84–94.

[7] W. Xie, X. Tong, J. Luo, Z. Deng, Q. Qi, Y. Chu, Design of Leachate concentrate treatment project based on DTZ evaporation, China Water Wastewater, 27 (2011) 56–60.
[8] D. Wang, D. Liu, Z. Gong, L. Tao, Q. Liu, Treatment of landfill Leachate reverse osmosis concentrate by Fenton oxidation-coagulation-adsorption, Sci. Technol. Eng., 13 (2013) 5423–5426.
[9] Z. Yuan, C. He, Q. Shi, C. Xu, Z. Li, C. Wang, H. Zhao, J. Ni, Molecular insights into the transformation of dissolved organic matter in landfill leachate concentrate during biodegradation and coagulation processes using ESI FT-ICR MS, Environ. Sci. Technol., 51 (2017) 8110–8118.
[10] Y. Long, J. Xu, D. Shen, Y. Du, H. Feng, Effective removal of contaminants in landfill leachate membrane concentrates by coagulation, Chemosphere, 167 (2017) 512–519.
[11] Y. Hu, Y. Lu, G. Liu, H. Luo, R. Zhang, X. Cai, Effect of the structure of stacked electro-Fenton reactor on treating nano-filtration concentrate of landfill leachate, Chemosphere, 202 (2018) 191–197.
[12] W. Chen, A. Zhang, Z. Gu, Q. Li, Enhanced degradation of refractory organics in concentrated landfill leachate by Fe^0/H_2O_2 coupled with microwave irradiation, Chem. Eng. J., 354 (2018) 680–691.
[13] H. Wang, Y. Wang, Z. Lou, N. Zhu, H. Yuan, The degradation processes of refractory substances in nanofiltration concentrated leachate using micro-ozonation, Waste Manage., 69 (2017) 274–280.
[14] T. Zhou, T.T. Lim, S.S. Chin, A.G. Fane, Treatment of organics in reverse osmosis concentrate from a municipal wastewater reclamation plant: feasibility test of advanced oxidation processes with/without pretreatment, Chem. Eng. J., 166 (2011) 932–939.
[15] N. Amaral-Silva, R.C. Martins, C. Paiva, S. Castro-Silva, R.M. Quinta-Ferreira, A new winery wastewater treatment approach during vintage periods integrating ferric coagulation, Fenton reaction and activated sludge, J. Environ. Chem. Eng., 4 (2016) 2207–2215.
[16] A. Yazdanbakhsh, F. Mehdipour, A. Eslami, H.S. Maleksari, F. Ghanbari, The combination of coagulation, acid cracking and Fenton-like processes for olive oil mill wastewater treatment: phytotoxicity reduction and biodegradability augmentation, Water Sci. Technol., 71 (2015) 1097–1105.
[17] N. Jaafarzadeh, F. Ghanbari, M. Alvandi, Integration of coagulation and electro-activated HSO_5^- to treat pulp and paper wastewater, Sustainable Environ. Res., 27 (2017) 223–229.
[18] H. Wang, C. Le, Study on the treatment of concentrated water from nanofiltration of bio-treated landfill leachate by coagulation–sedimentation and Fenton oxidation process, Guangdong Chem. Ind., 43 (2016) 116–117.
[19] Z. An, X. Xu, Treatment of membrane concentrated "young" landfill leachate by coagulation sedimentation, Adv. Mater. Res., 634–638 (2013) 349–352.
[20] J. Huang, J. Chen, Z. Xie, X. Xu, Treatment of nanofiltration concentrates of mature landfill leachate by a coupled process of coagulation and internal micro-electrolysis adding hydrogen peroxide, Environ. Technol., 36 (2015) 1001–1007.
[21] S. Renou, J.G. Givaudan, S. Poulain, F. Dirassouyan, P. Moulin, Landfill leachate treatment: review and opportunity, J. Hazard. Mater., 150 (2008) 468–493.
[22] K.E. Lee, N. Morad, T.T. Teng, B.T. Poh, Development, characterization and the application of hybrid materials in coagulation/flocculation of wastewater: a review, Chem. Eng. J., 203 (2012) 370–386.
[23] S. Ghafari, H.A. Aziz, M.H. Isa, A.A. Zinatizadeh, Application of response surface methodology (RSM) to optimize coagulation-flocculation treatment of leachate using poly-aluminum chloride (PAC) and alum, J. Hazard. Mater., 163 (2009) 650–656.
[24] J. Xu, Y. Long, D. Shen, H. Feng, T. Chen, Optimization of Fenton treatment process for degradation of refractory organics in pre-coagulated leachate membrane concentrates, J. Hazard. Mater., 323 (2017) 674–680.
[25] APHA, Standard Methods for the Examination of Water and Wastewater, 21st ed., American Public Health Association, Washington, DC, 2005.

[26] B. Lai, H. Qin, Y. Zhou, C. Pang, J. Xu, Y. Lian, S. Zhang, J. Zhou, Rapid detection of the degradation of the typical pollutants from ABS wastewater using Fourier transform infrared spectroscopy, Acta Opt. Sin., 2 (2011) 268–273.

[27] A. Baker, D. Ward, S.H. Lieten, R. Periera, E.C. Simpson, M. Slater, Measurement of protein-like fluorescence in river and wastewater using a handled spectrophotometer, Water Res., 38 (2004) 2934–2938.

[28] J.M. Duan, J. Gregory, Coagulation by hydrolyzing metal salts, Adv. Colloid Interface Sci., 100–102 (2003) 475–502.

[29] M. Vedrenne, R. Vasquez-Medrano, D. Prato-Garcia, B.A. Frontana-Uribe, J.G. Ibanez, Characterization and detoxification of a mature landfill leachate using a combined coagulation–flocculation/photo Fenton treatment, J. Hazard. Mater., 205–206 (2012) 208–215.

[30] W. Lee, P. Westerhoff, Dissolved organic nitrogen removal during water treatment by aluminum sulfate and cationic polymer coagulation, Water Res., 20 (2006) 3767–3774.

[31] W. Chen, Z. Gu, P. Wen, Q. Li, Degradation of refractory organic contaminants in membrane concentrates from landfill leachate by a combined coagulation-ozonation process, Chemosphere, 217 (2019) 411–422.

[32] A.A. Ahmad, B.H. Hameed, Effect of preparation conditions of activated carbon from bamboo waste for real textile wastewater, J. Hazard. Mater., 173 (2010) 487–493.

[33] M. Moradi, F. Ghanbari, E. Minaee Tabrizi, Removal of acid yellow 36 using Box–Behnken designed photoelectro-Fenton: a study on removal mechanisms, Toxicol. Environ. Chem., 97 (2015) 700–709.

[34] V. Kanokkantapong, T. Marhaba, B. Panyapinyophol, P. Pavasant, FTIR evaluation of functional groups involved in the formation of haloacetic acids during the chlorination of raw water, J. Hazard. Mater., 136 (2006) 188–196.

[35] W. Chen, P. Westerhoff, J.A. Leenheer, K. Booksh, Fluorescence excitation-emission matrix regional integration to quantify spectra for dissolved organic matter, Environ. Sci. Technol., 37 (2003) 5701–5710.

[36] L. Bu, K. Wang, Q. Zhao, L. Wei, J. Zhang, J. Yang, Characterization of dissolved organic matter during landfill leachate treatment by sequencing batch reactor, aeration corrosive cell-Fenton, and granular activated carbon in series, J. Hazard. Mater., 179 (2010) 1096–1105.